

Numerical analysis of the effect of the evaporator inlet-outlet position on the PV-T performance

Evaporatör giriş-çıkış konumunun PV-T performansı üzerindeki etkisinin sayısal analizi

Rıdvan YAKUT *¹ 

¹ Department of Mechanical Engineering, Kafkas University, Kars 36100, Turkey

• Received: 10.04.2022

• Accepted: 30.11.2022

Abstract

The increase in global energy consumption and carbon dioxide emissions increase the interest in renewable energy sources. Solar energy is at the forefront of renewable energy sources, and the decrease in cell efficiency due to various reasons during operation is an obstacle to this technology. Increasing the temperature of photovoltaic cells during operation causes a decrease in cell efficiency. Control of photovoltaic cells temperature is crucial in terms of both prolonging the economic life of the cells and increasing the efficiency of the system. The effect of the evaporator inlet and outlet position of the fluid on the heat transfer is known, but this effect was not examined in the studies carried out to increase the efficiency of the PV-T (photovoltaic-thermal) system. In the current study, the system efficiency parameters and COP (coefficient of performance) values of a PV-T evaporator cooled by forced air circulation were investigated by CFD (computational fluid dynamics) analysis. The analyzes were carried out in a single array for three different flow rates (0.0125 kg/s, 0.0250 kg/s, 0.0500 kg/s) and nine different evaporator inlet-outlet positions (CC, CL, CR, RC, RL, RR, LC, LL, LR), constant radiation of 1000 W/m². It was determined that there is a total efficiency difference of over 20% and an overall COP difference of over 25% between the best and worst inlet-outlet positions. The highest total and thermal efficiency were obtained for the RR condition, and the highest electrical efficiency was obtained for the LR condition but in the long-term, the highest efficiency can be achieved with the LC design. In the study also the highest COP values were calculated for the CL condition and the worst COP values for the RR condition.

Keywords: CFD, COP, Electrical efficiency, Photovoltaic thermal collectors, Thermal efficiency

Öz

Küresel enerji tüketimindeki ve karbondioksit emisyonlarındaki artış, yenilenebilir enerji kaynaklarına olan ilgiyi artırmaktadır. Yenilenebilir enerji kaynaklarının başında güneş enerjisi gelmektedir ve çalışma esnasında çeşitli sebeplerle hücre verimliliğinin düşmesi bu teknolojinin önündeki engeldir. Fotovoltaik hücrelerin çalışma sırasında sıcaklığının artması hücre veriminin düşmesine neden olmaktadır. Fotovoltaik hücre sıcaklığının kontrolü hem hücrelerin ekonomik ömrünü uzatmak hem de sistemin verimini artırmak açısından çok önemlidir. Akışkanın buharlaştırıcıya giriş ve çıkış konumunun ısı transferine etkisi bilinmektedir ancak PV-T (fotovoltaik-termal) sisteminin verimini artırmak için yürütülen çalışmalarda bu etki incelenmemiştir. Bu çalışmada, cebri hava sirkülasyonu ile soğutulan bir PV-T evaporatörün sistem verimlilik parametreleri ve COP (performans katsayısı) değerleri, HAD (hesaplamalı akışkanlar dinamiği) analizi ile incelenmiştir. Analizler, tek dizide, üç farklı debide (0.0125 kg/s, 0.0250 kg/s, 0.0500 kg/s), dokuz farklı buharlaştırıcıya giriş-çıkış pozisyonu (CC, CL, CR, RC, RL, RR, LC, LL, LR) ve 1000 W/m² sabit radyasyon için yürütülmüştür. En iyi ve en kötü giriş-çıkış konumları arasında %20'nin üzerinde bir toplam verimlilik farkı ve %25'in üzerinde bir genel COP farkı olduğu belirlenmiştir. En yüksek toplam ve termal verim RR koşulu için, en yüksek elektriksel verim LR koşulu için elde edilmiştir ancak uzun vadede en yüksek verim LC tasarımı ile elde edilebilmektedir. Çalışmada ayrıca CL koşulu için en yüksek COP değerleri ve RR koşulu için en kötü COP değerleri hesaplanmıştır.

Anahtar kelimeler: HAD, COP, Elektriksel verim, Fotovoltaik termal sistem, Termal verim

* Rıdvan Yakut: r_yakut@yahoo.com

1. Introduction

In the last two centuries, factors such as industrialization, urbanization, and human population growth cause an upsurge in global energy consumption. Nowadays, 80% of the global energy demand is provided by fossil fuels and it is expected to increase by 48% in the next 20 years (Moodley, 2021). As a result of fossil fuels combustion, which is a non-renewable energy source and contains high levels of carbon, harmful and polluting gases such as carbon dioxide, carbon monoxide, nitrogen, sulfur oxide are released and mixed with the atmosphere. The approximately two-fold increase in atmospheric carbon dioxide concentration in the last century caused the world temperature to increase by more than 1 °C (Morice et al., 2012; Ritchie & Roser, 2020). The increase in atmospheric carbon dioxide levels causes an increase in the greenhouse effect and global warming. The biggest source of sector-based global greenhouse gas emissions is energy consumption (Ritchie & Roser, 2020). Due to global warming, the life of all living things in the world is in danger, and many plant and animal species are in danger of extinction. For a cleaner environment and a more livable world, energy sources must be converted to renewable energy sources. Currently, the most used renewable energy sources are solar, wind, geothermal, bio-power, and hydropower. Solar power is the most abundant and the cleanest renewable energy source in use around the world and is becoming increasingly popular for generating electricity.

Solar energy is based on the principle of converting the energy carried by photons from the sun into electrical energy with photovoltaic systems. The essential energy range for photovoltaic cells to generate voltage is 0-1.12 eV (Masters, 2004). Therefore, PV (photovoltaic) systems can convert a limited part of the radiation coming to its surface into electrical energy. The photon above this energy range is stored as heat in the system and causes a decrease in system efficiency and materials lifespan (Kandilli et al., 2013; Omeroğlu, 2018). On the other hand, PV-T systems eliminate these disadvantages in PV systems, remove the heat load above the energy level from the system and enable it to be used as thermal energy. Although PV-T systems are a good method for converting solar energy, their efficiency decreases due to reflection (15%), absorption (5%), and poor insulation (~45%) (Rahman et al., 2018). Many studies were carried out in the literature to eliminate these losses.

Abdullah et al. (2019) reported that researches on channel/collector depth (Delfani et al., 2019) and length (Do Ango et al., 2013), number of collectors (Zadeh et al., 2015), solar tracking system (Rizk & Chaiko, 2008), absorber plate design parameters (tube diameter (Kim & Seo, 2007), tube spacing (Ghamari & Worth, 1992), fin thickness (Pottler et al., 1999)), booster diffuse reflector (Tripanagnostopoulos et al., 2002), collector tilt angle (Handoyo & Ichسانی, 2013), PV module type (Jiang et al., 2011), glass thickness (Bakari et al., 2014), glazing material (Dondapati et al., 2018), anti-reflective coating (Ali et al., 2014), riser-header configuration (Zwalnan et al., 2021), riser location (Ekramian et al., 2014), thermal conductivity of tedlar (Koech et al., 2012), thermal insulation (Kehrer et al., 2003), absorber material (Kennedy, 2002), absorber thickness (Belaidi et al., 2008), fins (Ozakin et al., 2020), multi-inlet (Hassan & Abo-Elfadl, 2018), PV cell material (Dhass et al., 2020), solar radiation (Hamrouni et al., 2008), relative humidity (Ettah et al., 2012), wind speed (Ozakin & Kaya, 2019), ambient temperature (Alshawaf et al., 2020), accumulated dust (Adinoyi & Said, 2013), mass flow rate (Yakut, 2021), thermal resistance (Zondag, 2008), inlet and outlet temperatures (Richert et al., 2015), heat loss coefficient (Sekhar et al., 2009), heat removal factor (Malvi et al., 2017), packing factor (Ji et al., 2006), and effect of fan (Arslan et al., 2020) were carried out in the literature to improve the performance of solar systems (Abdullah et al., 2019). In addition to all these effects, the effects of parameters such as fluid type (Atmaca & Pektemir, 2020), absorber plate (Atmaca & Pektemir, 2019a) and glass cover properties (Atmaca & Akiskalioglu, 2020) on the efficiency of PV-T systems were investigated. Although the effects of many parameters were examined in these studies, the effect of fluid inlet and outlet positions on system performance was not examined. However, the decrease in the operating temperatures of photovoltaic systems increases the cell efficiency and the fluid inlet-outlet positions are effective on heat transfer (Chein & Chen, 2009; Fesharaki et al., 2011). In this study, the effect of the input and output positions of the fluid to the solar collector was investigated numerically.

The effect of many parameters examined in studies on solar systems can be determined numerically, but the effect of constantly changing environmental conditions such as relative humidity, solar radiation, ambient temperature, wind speed, and accumulated dust cannot be determined (Abdullah et al., 2019). Moreover, solar system efficiency decreases in long-term because photovoltaic cells are exposed to sunlight for a long time (Chegaar et al., 2004; Cuce & Cuce, 2014; Cuce et al., 2013; Du et al., 2012). Therefore, it is difficult to

determine the system efficiency with high numerical accuracy. These effects should be taken into account when determining the amortization periods of solar systems (Ozakin et al., 2020). Numerical analyzes provide more economical solutions in a short time compared to experimental studies although there are many uncertainties in the numerical determination of the efficiency of solar systems. Another advantage of numerical analysis is that the variables on the system can be adapted much more easily than the experimental process. In addition, analytically difficult or impossible problems are solved easily. For this reason, CFD is crucial to calculate with high accuracy the effects of operating and basic design parameters on solar system performance (Kalkan et al., 2019).

In the literature, most of the numerical studies are 1D or 2D studies with low computational performance, and erroneous predictions are made because PV temperature is neglected in the airflow direction (Kalkan et al., 2019). In the current study, a steady-state 3D numerical model was developed in the ANSYS-FLUENT program, and in-line array heat sinks were used to evaluate the heat transfer properties of a PV-T system. The present study is the first in the literature to examine the effect of fluid inlet - outlet position on PV-T panel performance. Numerical simulations are carried out to determine the effect of operating conditions (mass flow rate), and design parameters of the PV-T system (evaporator inlet-outlet position). Analysis results are presented the total, thermal and electrical efficiency of the PV-T evaporator, thermal and overall coefficient of performance, temperature and velocity contours.

2. Computational model

The numerical model simulated and analyzed in ANSYS Fluent program to determine the effect of input-output position on PV-T system performance is shown in Figure 1. Since the PV evaporator (1.6×1 m) geometry is suitable for symmetrical modeling, a semi-symmetrical model was created. The advantage of the symmetric model over the full model is that it allows more grids to be created on the geometry and to be calculated in a shorter time.

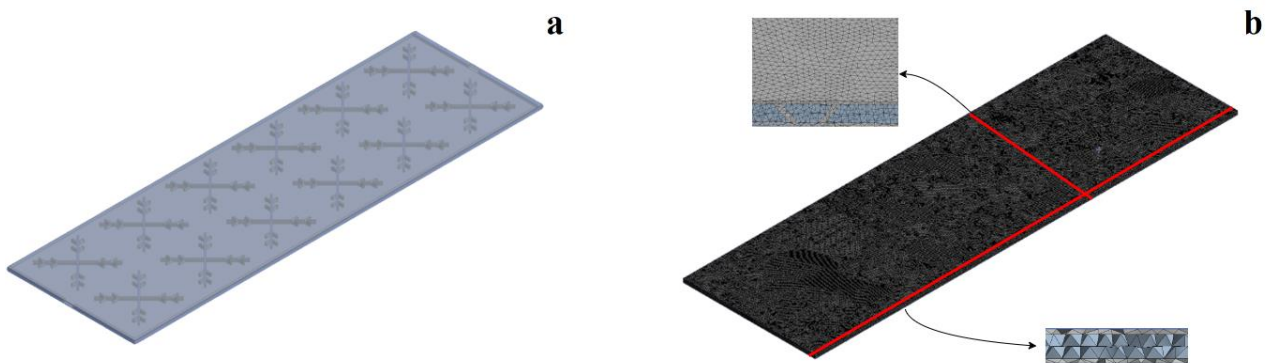


Figure 1. (a) Solid geometry, (b) Mesh structure of PV evaporator

Air was used as the fluid in the study because of its low corrosive character (Atmaca & Pektemir, 2019b). In the current study, snowflake heat sinks were used to remove the heat from the evaporator. The variables of the heat sinks in the numerical study are given in Figure 2.

PV-T evaporator solid model was generated in nine evaporator inlet – outlet position (CC, RC, LC, CR, RR, LR, CL, RL, LL). The part shown with the dashed line in Figure 3 is the symmetry axis, thus the inlet-outlet from the left part is from the middle of the whole evaporator. The names of the input and output positions are abbreviated as shown in Figure 3.

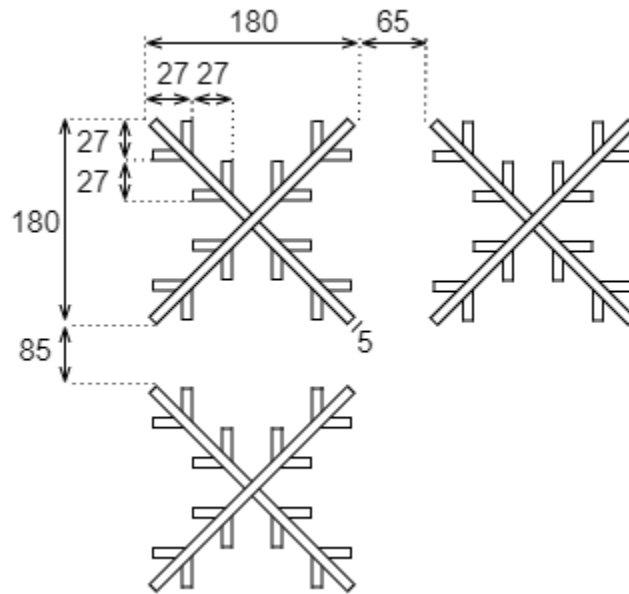


Figure 2. Snowflake heat sink

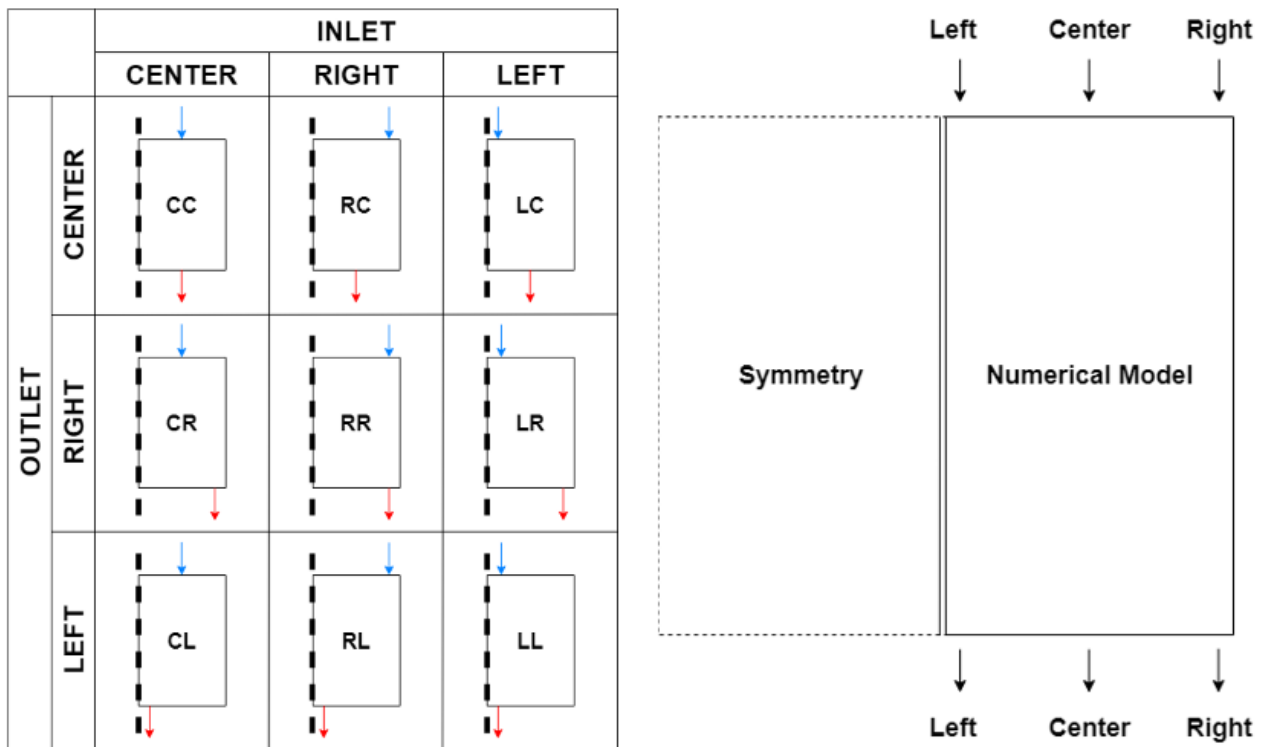


Figure 3. Inlet and outlet positions of the fluid to the PV evaporator

Grid quality is significant for convergence of analyzes. Although there are many grid quality parameters, the most important parameters are skewness, aspect ratio and orthogonal quality. In the numerical analysis, it is not desired for the aspect ratio to exceed 20, for the skewness value to approach 1, and for the orthogonal quality to approach 0 (Ansys, 2009). Grid quality increases with increasing grid number, but not always. In addition, the increase in the number of grids causes an increase in the solution times and a heavy load on the processor. For this reason, it is necessary to perform grid independence analyzes in numerical analysis. In the current study, grid independence analyzes were performed for the model and optimum grid number was determined as 587104. Table 1 shows the mesh qualities and the results obtained in the grid independence studies.

Table 1. Grid independence analyzes results

	Mesh I	Mesh II	Mesh III	Mesh IV
Number of Elements	314982	587104	930614	1589264
Aspect Ratio	3.05	2.46	2.23	2.00
Skewness	0.51	0.41	0.37	0.29
Orthogonal Quality	0.48	0.59	0.63	0.71
Mean Velocity in Channel	2.88	3.24	3.24	3.4
Temperature	318	316	317	316

The realizable $k - \varepsilon$ model exhibits high-performance for strong streamline curvature, rotation, and vortex flows compared to other methods (Fluent, 2013). Therefore, $k - \varepsilon$ model was used as the turbulence model. Enhanced wall treatment was used as near-wall treatment option. The convergence criterion was set at 10^{-6} for energy equation, and 1000 iterations were applied to converge. The boundary conditions of the numerical model are shown in Table 2.

Table 2. Boundary conditions

Model	Symmetry
Fluid	Air
Heat Flux (W/m^2)	1000
Flow Rate (kg/s)	0.0125-0.0250-0.0500
Outlet	Pressure outlet
Number of Iterations	1000
Number of Grids	~ 600000

3. Calculations

3.1. Governing equations

Three-dimensional continuity, energy and momentum equations for steady state turbulent flow in Cartesian coordinates are solved in ANSYS Fluent program. These conservation equations are defined below (Ansys, 2009; Yang & Peng, 2009).

Continuity equation

$$\frac{\partial \rho \bar{u}_i}{\partial x_i} = 0 \quad (1)$$

Momentum equation

$$\rho \bar{u}_j \frac{\partial \bar{u}_i}{\partial x_j} = -\frac{\partial \bar{p}}{\partial x_i} + \frac{\partial}{\partial x_j} \left[\mu_t \left(\frac{\partial \bar{u}_i}{\partial x_j} + \frac{\partial \bar{u}_j}{\partial x_i} \right) \right] \quad (2)$$

Energy equation

$$\rho \bar{u}_j \frac{\partial \bar{T}}{\partial x_j} = -\frac{\partial}{\partial x_j} \left[\left(\frac{\mu_l}{\sigma_l} + \frac{\mu_t}{\sigma_t} \right) \frac{\partial \bar{T}}{\partial x_j} \right] \quad (3)$$

Transport equation for k

$$\rho \bar{u}_j \frac{\partial k}{\partial x_j} = \frac{\partial}{\partial x_j} \left(\frac{\mu_t}{\sigma_k} \frac{\partial k}{\partial x_j} \right) + \mu_t \left(\frac{\partial \bar{u}_i}{\partial x_j} + \frac{\partial \bar{u}_j}{\partial x_i} \right) \frac{\partial \bar{u}_i}{\partial x_j} - \rho \varepsilon \quad (4)$$

Transport equation for ε

$$\rho \bar{u}_j \frac{\partial \varepsilon}{\partial x_j} = \frac{\partial}{\partial x_j} \left(\frac{\mu_t}{\sigma_\varepsilon} \frac{\partial \varepsilon}{\partial x_j} \right) + C_1 \mu_t \frac{\varepsilon}{k} \left(\frac{\partial \bar{u}_i}{\partial x_j} + \frac{\partial \bar{u}_j}{\partial x_i} \right) \frac{\partial \bar{u}_i}{\partial x_j} - C_2 \rho \frac{\varepsilon^2}{k} \quad (5)$$

The constants in the equations are turbulent viscosity (μ_t), kinetic energy (k), dissipation rate (ε). σ_k and σ_ε are turbulent Prandtl number for k and epsilon, respectively. The values of the empirical constants (C_μ , C_1 , C_2) in the equation are $\sigma_k = 1.0$, $\sigma_\varepsilon = 1.3$, $C_\mu = 0.09$, $C_1 = 1.44$, $C_2 = 1.92$.

3.2. Efficiency calculations

For the calculation and design of today's modern engineering structures, many computer programs have been developed that enable the transfer of results to application projects in an integrated manner and facilitate data transfer. In this study, Seismostruct software was used (Seismosoft, 2022). While determining the effect of local soil conditions on structural performance, an 8-storey reinforced concrete structure was chosen. As an example, the floor plan of a reinforced concrete building is shown in Figure 3. There are four spans in both the X and Y directions and each span is chosen as 4 m.

The total efficiency of a PV-T system (η_{PV-T}) is equal to the sum of the electrical efficiency (η_{PV}) and the thermal efficiency (η_T), and is expressed as follows:

$$\eta_{PV-T} = \eta_{PV} + \eta_T \quad (6)$$

The thermal efficiency of the PV-T system (η_T) is stated as

$$\eta_T = \frac{\dot{Q}_a}{A_{PV} \times I} \quad (7)$$

A_{PV} , and I are collector area and radiation, respectively. \dot{Q}_a is the heat absorbed by the evaporator and is expressed as the difference between the thermal power of the heat transfer fluid at the inlet and outlet of the collector as follows (Alessandro et al., 2021)

$$\dot{Q}_a = \dot{m} C_p (T_o - T_i) \quad (8)$$

where \dot{m} , C_p , T_o , and T_i respectively represent mass flow rate, specific heat of fluid, outlet and inlet fluid temperatures.

The electrical efficiency of PV cells (η_{PV}) can be defined by the following expression.

$$\eta_{PV} = \frac{V_{\max} \times I_{\max}}{A_{PV} \times I} \quad (9)$$

V_{\max} and I_{\max} represent maximum voltage and maximum current, respectively. The present study was carried out numerically and it is not possible to determine the voltage and current values for the PV-T system. Therefore, the following equation developed by Evans (Evans, 1981) was used to determine the electrical efficiency of the PV cells (η_{PV}).

$$\eta_{PV} = \eta_{\text{ref}} [1 - \beta (T_{PV} - T_{\text{ref}})] \quad (10)$$

where η_{ref} is the reference efficiency ($\eta_{\text{ref}} = 0.12$) under standard conditions. In this study, the standard conditions are 1000 W/m^2 and $25 \text{ }^\circ\text{C}$. β is the thermal coefficient for cell efficiency and here the value determined for silicon cells ($\beta = 0.00045/\text{K}$) is taken (Joshi et al., 2009; Nahar et al., 2017). T_{PV} and T_{ref} respectively represent cell and reference temperature.

3.3. COP calculations

The thermal coefficient of performance (COP_T) for the PV-T system was calculated from the equation below.

$$COP_T = \frac{\dot{Q}_A}{\dot{Q}_C} \quad (11)$$

\dot{Q}_A and \dot{Q}_C represent the heat absorbed by the evaporator and power consumption of the PV-T system, respectively. Classic heat pump only generates heat, Therefore COP is calculated by Eq. 11, but photovoltaic heat pump can produce electricity (\dot{Q}_{PV}) in addition to heat, therefore the overall coefficient of performance for the PVT system (COP_{PVT}) is defined by the following equation (Lu et al., 2019; Song et al., 2021; Zhang et al., 2014; Zhou et al., 2016). In the current study, the \dot{Q}_{PV} and \dot{Q}_C values were obtained from the study conducted in literature (Lu et al., 2019).

$$COP_{PVT} = \frac{\dot{Q}_A + \dot{Q}_{PV}/0.38}{\dot{Q}_C} \quad (12)$$

4. Results

4.1. Evaporator inlet – outlet position contours

Figure 4 shows the temperature and velocity contours of nine different evaporator inlet-outlet locations at a flow rate of 0.025 kg/s. Similar velocity and temperature distributions were obtained at other flow rates, thus only the velocity and temperature distributions at 0.025 kg/s flow rate are presented. It is seen in the figure that the most homogeneous velocity distribution is in LL. In this case, the fluid passed through almost every space with equal flow and caused a flow with a homogeneous velocity distribution, without high-speed flow along the channel. The homogeneity of the flow is important both in terms of preventing the formation of high-temperature zones on the panel and in preventing the abrasion of the fins in long-term use. It is seen that the flow of the fluid from the left side ensures a more controlled and homogeneous flow of the fluid. In cases where the fluid enters from the center, it is seen that the flow velocity is very high on the main channel. Although this situation is well reflected in the temperature contours, it will cause wear of the heat sinks and cavitation in long-term use. In the conditions where the fluid enters from the center and the outlet is on the right and left, it is seen that there is almost no flow in the opposite direction of the outlet. For this reason, the surface temperature increased in these regions where there is no flow. In cases where the fluid enters from the right, it is seen that the fluid reaches some areas on the left side of the channel very little and some areas do not reach it at all. This causes the flow rate to be very high on the right side and very low on the left side, and because the fluid does not reach the left side of the panel, it causes the formation of high-temperature contours.

It is seen in the Figure 4 that the most homogeneous temperature distribution is at CC. In CR and CL, the temperature distribution is similar and the mean surface temperature is very close to each other. It is seen that high-temperature regions do not occur with the inlet of the fluid from the left side. In the cases where the fluid enters from the left side, the temperature distributions are very similar, but the minimum mean surface temperature was LR. It is seen that the flow of the fluid from the right side prevents homogeneous temperature distribution. This is because the fluid enters from the right side and cannot reach the left side due to the structure of the fins. The highest temperature region was formed in the RR. In this case, the fluid is confined to the right side only, thus the left side is not sufficiently cooled. According to the temperature contours obtained as a result of the analysis, it can be said that since high-temperature zones are not formed in the CC, LC, LR, LL designs, it can enable the photovoltaic cells to work for a long-term at the optimum operating temperature.

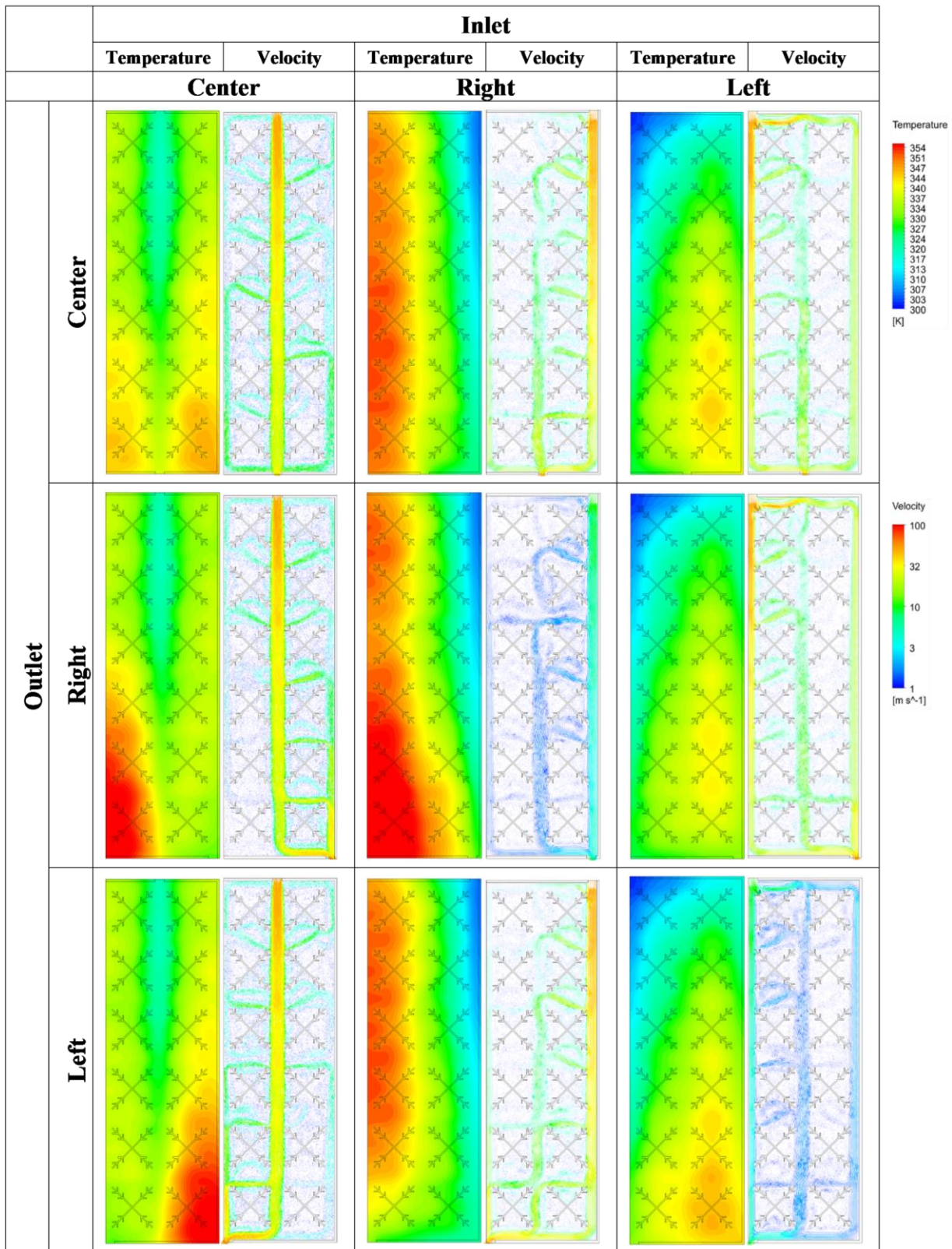


Figure 4. Temperature contours and velocity vectors for a flow rate of 0.025 kg/s

4.2. Efficiency results

Figure 5 presents the thermal, electrical and total efficiency of the PV system. The figure clearly shows the effects of the evaporator inlet and outlet position of the fluid on the efficiency. In all three flow rates, the highest total and thermal efficiency were obtained for the RR condition, and the highest electrical efficiency was obtained for the LR condition. Total and thermal efficiency remained almost the same except for the CC

flow condition. The electrical efficiency increased with the increase in flow rate. Between the minimum and maximum flow rate, there was an increase in electrical efficiency of 25-30%. The decrease in mean surface temperature resulted in an increase in electrical efficiency. It has been determined that the effect of the evaporator inlet and outlet position of the fluid on the electrical efficiency is greater at low flow rates, while the effect decreases as the mean surface temperatures close to each other with the increase in flow rate. Since the thermal efficiency is higher in the cases where the fluid enters from the right and the electrical efficiency of the PV cells is limited, it has ensured that the total efficiency is higher than other conditions. However, considering the temperature and velocity contours presented in Figure 4, the flow of the fluid from the right-side causes both the unbalanced flow in the panel and the formation of high-temperature zones. For this reason, although the inflow of the fluid from the right side ensures that the thermal efficiency of the system is high in the short term, it will cause both the evaporator elements to wear faster in the long-term and the efficiency of the PV cells, which are constantly exposed to high temperatures, to decrease much more. Although the efficiency of the CC design increases with the increasing flow rate and provides homogeneous heat distribution, it will cause wear of the evaporator elements in the long-term due to the fact that the fluid reaches very high velocities in some areas in the channel. Therefore, in the long-term, the highest efficiency can be achieved with the LC design.

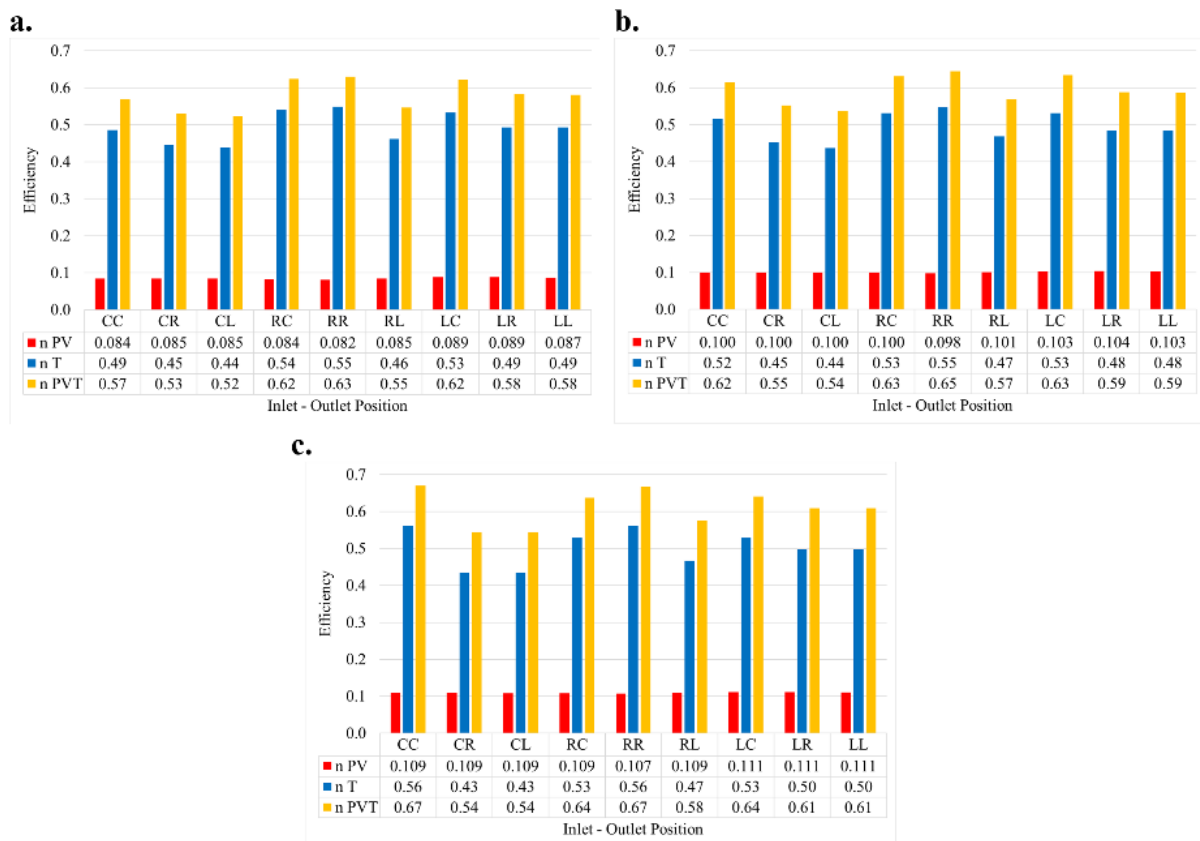


Figure 5. The effect of the evaporator inlet and outlet position on thermal, electrical, and total efficiency for a flow rate of (a) 0.0125 kg/s (b) 0.0250 kg/s (c) 0.0500 kg/s

4.3. COP results

Figure 6 shows the variation of the thermal and overall coefficient of performance of the system with increasing flow rate and evaporator inlet-outlet position. The results showed that the evaporator inlet and outlet position of the fluid affects the COP values. It was observed that the changes in thermal and overall COP values were similar to each other. It was determined that the difference between the highest and lowest thermal and overall COP values was around 25% in all three flow rates. Similar results were obtained for all three flow rates under all conditions except the CC condition. It has been observed that the COP calculated in the CC design decreases with the increase in flow rate. The highest COP values were calculated for the CL condition and the worst COP values for the RR condition. The results showed that the central entry of the fluid is a good way to achieve high COP values. Although LC was determined as the best design when the efficiencies and temperature–

velocity contours were evaluated, it was observed that the COP values were low. When evaluated together with COP values and temperature–velocity contours, it is seen that the most efficient design is the CL design, although it includes high temperature contours.

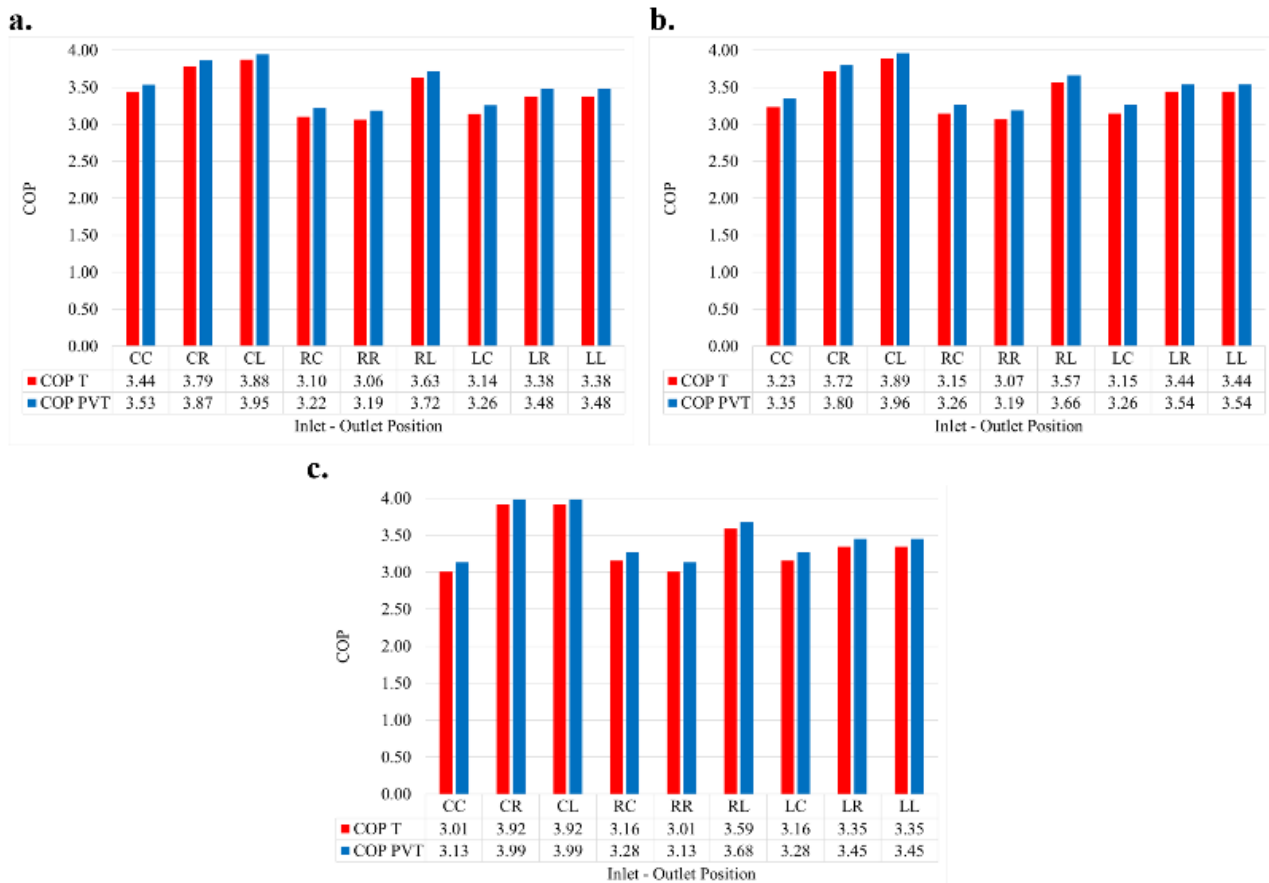


Figure 6. The effect of the evaporator inlet and outlet position on the COP values for a flow rate of (a) 0.0125 kg/s (b) 0.0250 kg/s (c) 0.0500 kg/s

5. Discussion and conclusions

Although the effect of many parameters to increase the efficiency of PV-T systems are examined in the literature, the effect of the evaporator inlet and outlet positions of the fluid in the PV-T evaporator is not examined. Present paper has a significant reference value for related studies. In the present numerical study, the effect of fluid inlet and outlet positions on PV-T system performance was investigated at three flow rates. The following conclusions could be drawn:

- The velocity and temperature contours showed that the evaporator inlet and outlet positions of the fluid have a crucial effect on the flow and temperature characteristics. In the ideal PV-T evaporator; (I) the fluid should pass through all channels, (II) there should be homogeneous velocity distribution, and (III) high-temperature zones should not occur. The fact that the flow is not homogeneous causes both the fluid to flow at a high velocity in a certain region and the temperature to increase in places where there is no flow. High temperature causes the efficiency of the PV cells to decrease in the long term, and the high velocity causes the evaporator elements to wear out over time.
- As a result of the analysis, the lowest surface temperature was reached in the LR condition. Analysis results show that the entrance of the fluid from the left side has a positive effect on the heat transfer, but when it enters from the right side, it affects the heat transfer badly since it cannot reach the left side of the evaporator.
- According to the velocity contours obtained as a result of the analysis, the most homogeneous velocity distribution was obtained in the LL state. It has been observed that when the fluid enters from the left side, flow occurs from almost every channel, and when it enters from the right side, the fluid cannot reach the

left side. When the fluid enters from the center, it has been observed that it reaches very high velocities on the mainline.

- In all three flow rates, the highest total and thermal efficiency were obtained for the RR condition, and the highest electrical efficiency was obtained for the LR condition. However, since the most homogeneous velocity and temperature conditions are provided by the LC condition, both velocity and temperature-related wear can be kept at a minimum in the long run and the highest efficiency can be obtained.
- It was determined that the difference between the highest and lowest thermal and overall COP values was around 25% in all three flow rates. The highest COP values were calculated for the CL condition and the worst COP values for the RR condition. The results showed that the central entry of the fluid is a good way to achieve high COP values.

In future work,

This study, in which the effect of evaporator inlet and outlet position on efficiency and COP is determined numerically, will be carried out experimentally. The effect of inlet and outlet dimensions in the experimental set to be established will also be examined.

Author contribution

The author provided the literature review of the article, the preparation and analysis of the model, the preparation of all figures and tables, and the evaluation of the results.

Declaration of ethical code

The author declare that he has no known competing financial interests or personal relationships that could have appeared to influence the work reported in this paper.

Conflicts of interest

The authors declare that they have no conflict of interest.

References

- Abdullah, A. L., Misha, S., Tamaldin, N., Rosli, M. A. M., & Sachit, F. A. (2019). A Review: Parameters affecting the PVT collector performance on the thermal, electrical, and overall efficiency of PVT system. *Journal of Advanced Research in Fluid Mechanics and Thermal Sciences*, 60(2), 191-232. <https://akademiabaru.com/submit/index.php/arfmts/article/view/2643/1707>
- Adinoyi, M. J., & Said, S. A. M. (2013). Effect of dust accumulation on the power outputs of solar photovoltaic modules. *Renewable Energy*, 60, 633-636. <https://doi.org/10.1016/j.renene.2013.06.014>
- Alessandro, M., Niccolao, A., & Fabrizio, L. (2021). Photovoltaic-thermal solar-assisted heat pump systems for building applications: Integration and design methods. *Energy and Built Environment*. <https://doi.org/10.1016/j.enbenv.2021.07.002>
- Ali, K., Khan, S. A., & Jafri, M. Z. M. (2014). Effect of double layer (SiO₂/TiO₂) anti-reflective coating on silicon solar cells. *International Journal of Electrochemical Science*, 9(12), 7865-7874. <http://www.electrochemsci.org/papers/vol9/91207865.pdf>
- Alshawaf, M., Poudineh, R., & Alhajeri, N. S. (2020). Solar PV in Kuwait: The effect of ambient temperature and sandstorms on output variability and uncertainty. *Renewable and Sustainable Energy Reviews*, 134, 110346. <https://doi.org/10.1016/j.rser.2020.110346>
- Ansys, I. (2009). Ansys fluent 12.0 user's guide. *New Hampshire: Ansys Inc*, 35-47. https://www.afs.enea.it/project/neptunius/docs/fluent/html/ug/main_pre.htm

- Arslan, E., Aktaş, M., & Can, Ö. F. (2020). Experimental and numerical investigation of a novel photovoltaic thermal (PV/T) collector with the energy and exergy analysis. *Journal of Cleaner Production*, 276, 123255. <https://doi.org/10.1016/j.jclepro.2020.123255>
- Atmaca, M., & Akiskalioglu, E. (2020). PV/T sisteminde cam kapak özelliklerinin elektriksel ve termal verime etkilerinin araştırılması. *Bartın University International Journal of Natural and Applied Sciences*, 3(2), 52-65. <https://dergipark.org.tr/tr/pub/jonas/issue/57209/766617>
- Atmaca, M., & Pektemir, İ. Z. (2019a). PV panelinin altına serbest olarak yerleştirilen siyah emici plakanın termal kapasitesinin belirlenmesi. *International Journal of Advances in Engineering and Pure Sciences*, 31(4), 280-285. <https://doi.org/10.7240/jeps.470175>
- Atmaca, M., & Pektemir, İ. Z. (2019b). An investigation on the effect of the total efficiency of water and air used together as a working fluid in the photovoltaic thermal systems. *Processes*, 7(8), 516. <https://doi.org/10.3390/pr7080516>
- Atmaca, M., & Pektemir, İ. Z. (2020). Photovoltaic-thermal system for building application: A case study. *Energy Sources, Part A: Recovery, Utilization, and Environmental Effects*, 1-18. <https://doi.org/10.1080/15567036.2020.1817180>
- Bakari, R., Minja, R. J. A., & Njau, K. N. (2014). Effect of glass thickness on performance of flat plate solar collectors for fruits drying. *Journal of Energy*, 2014. <https://doi.org/10.1155/2014/247287>
- Belaidi, A., Dittrich, T., Kieven, D., Tornow, J., Schwarzburg, K., & Lux-Steiner, M. (2008). Influence of the local absorber layer thickness on the performance of ZnO nanorod solar cells. *Physica Status Solidi*, 2(4), 172-174. <https://doi.org/10.1002/pssr.200802092>
- Chegaar, M., Ouennoughi, Z., & Guechi, F. (2004). Extracting dc parameters of solar cells under illumination. *Vacuum*, 75(4), 367-372. <https://doi.org/10.1016/j.vacuum.2004.05.001>
- Chein, R., & Chen, J. (2009). Numerical study of the inlet/outlet arrangement effect on microchannel heat sink performance. *International Journal of Thermal Sciences*, 48(8), 1627-1638. <https://doi.org/10.1016/j.ijthermalsci.2008.12.019>
- Cuce, E., & Cuce, P. M. (2014). Improving thermodynamic performance parameters of silicon photovoltaic cells via air cooling. *International Journal of Ambient Energy*, 35(4), 193-199. <https://doi.org/10.1080/01430750.2013.793481>
- Cuce, E., Cuce, P. M., & Bali, T. (2013). An experimental analysis of illumination intensity and temperature dependency of photovoltaic cell parameters. *Applied Energy*, 111, 374-382. <https://doi.org/10.1016/j.apenergy.2013.05.025>
- Delfani, S., Esmaeili, M., & Karami, M. (2019). Application of artificial neural network for performance prediction of a nanofluid-based direct absorption solar collector. *Sustainable Energy Technologies and Assessments*, 36, 100559. <https://doi.org/10.1016/j.seta.2019.100559>
- Dhass, A. D., Kumar, R. S., Lakshmi, P., Natarajan, E., & Arivarasan, A. (2020). An investigation on performance analysis of different PV materials. *Materials Today: Proceedings*, 22, 330-334. <https://doi.org/10.1016/j.matpr.2019.06.005>
- Do Ango, A. C. M., Médale, M., & Abid, C. (2013). Optimization of the design of a polymer flat plate solar collector. *Solar Energy*, 87, 64-75. <https://doi.org/10.1016/j.solener.2012.10.006>
- Dondapati, R. S., Agarwal, R., Saini, V., Vyas, G., & Thakur, J. (2018). Effect of glazing materials on the performance of solar flat plate collectors for water heating applications. *Materials Today: Proceedings*, 5(14), 27680-27689. <https://doi.org/10.1016/j.matpr.2018.10.002>
- Du, B., Hu, E., & Kolhe, M. (2012). Performance analysis of water cooled concentrated photovoltaic (CPV) system. *Renewable and sustainable energy reviews*, 16(9), 6732-6736. <https://doi.org/10.1016/j.rser.2012.09.007>
- Ekramian, E., Etemad, S. G., & Haghshenasfard, M. (2014). Numerical analysis of heat transfer performance of flat plate solar collectors. *Journal of Fluid Flow, Heat and Mass Transfer (JFFHMT)*, 1, 38-42. <https://doi.org/10.11159/jffhmt.2014.006>
- Ettah, E. B., Udoimuk, A. B., Obiefuna, J. N., & Opara, F. E. (2012). The effect of relative humidity on the efficiency of solar panels in Calabar, Nigeria. *Universal Journal of Management and Social Sciences*, 2(3), 8-11.

<https://www.semanticscholar.org/paper/The-Effect-of-Relative-Humidity-on-the-Efficiency-Ettah-Udoimuk/55e0a5bbaca26d012ad99b0291240935813b47>

- Evans, D. L. (1981). Simplified method for predicting photovoltaic array output. *Solar Energy*, 27(6), 555-560. [https://doi.org/10.1016/0038-092X\(81\)90051-7](https://doi.org/10.1016/0038-092X(81)90051-7)
- Fesharaki, V. J., Dehghani, M., Fesharaki, J. J., & Tavasoli, H. (2011). The effect of temperature on photovoltaic cell efficiency. *Proceedings of the 1st International Conference on Emerging Trends in Energy Conservation* 1-6. https://research.iaun.ac.ir/pd/jfesharakiold/pdfs/PaperC_4124.pdf
- Fluent, A. (2013). Ansys fluent theory guide; Ansys Inc., Release, 15. https://www.afs.enea.it/project/neptunius/docs/fluent/html/th/main_pre.htm
- Ghamari, D. M., & Worth, R. A. (1992). The effect of tube spacing on the cost-effectiveness of a flat-plate solar collector. *Renewable Energy*, 2(6), 603-606. [https://doi.org/10.1016/0960-1481\(92\)90025-X](https://doi.org/10.1016/0960-1481(92)90025-X)
- Hamrouni, N., Jraidi, M., & Chérif, A. (2008). Solar radiation and ambient temperature effects on the performances of a PV pumping system. *Journal of Renewable Energies*, 11(1), 95-106. <https://www.asjp.cerist.dz/en/article/119583>
- Handoyo, E. A., & Ichsan, D. (2013). The optimal tilt angle of a solar collector. *Energy Procedia*, 32, 166-175. <https://doi.org/10.1016/j.egypro.2013.05.022>
- Hassan, H., & Abo-Elfadl, S. (2018). Experimental study on the performance of double pass and two inlet ports solar air heater (SAH) at different configurations of the absorber plate. *Renewable Energy*, 116, 728-740. <https://doi.org/10.1016/j.renene.2017.09.047>
- Ji, J., Han, J., Chow, T.-t., Yi, H., Lu, J., He, W., & Sun, W. (2006). Effect of fluid flow and packing factor on energy performance of a wall-mounted hybrid photovoltaic/water-heating collector system. *Energy and Buildings*, 38(12), 1380-1387. <https://doi.org/10.1016/j.enbuild.2006.02.010>
- Jiang, H., Lu, L., & Sun, K. (2011). Experimental investigation of the impact of airborne dust deposition on the performance of solar photovoltaic (PV) modules. *Atmospheric Environment*, 45(25), 4299-4304. <https://doi.org/10.1016/j.atmosenv.2011.04.084>
- Joshi, A. S., Tiwari, A., Tiwari, G. N., Dincer, I., & Reddy, B. V. (2009). Performance evaluation of a hybrid photovoltaic thermal (PV/T)(glass-to-glass) system. *International Journal of Thermal Sciences*, 48(1), 154-164. <https://doi.org/10.1016/j.ijthermalsci.2008.05.001>
- Kalkan, C., Ezan, M. A., Duquette, J., Yilmaz Balaman, Ş., & Yilanci, A. (2019). Numerical study on photovoltaic/thermal systems with extended surfaces. *International Journal of Energy Research*, 43(10), 5213-5229. <https://doi.org/10.1002/er.4477>
- Kandilli, C., Külahlı, G., & Savcı, G. (2013). *Fotovoltaik termal (PVT) sistem 2D termodinamik modellenmesi ve deneysel sonuçlarla karşılaştırılması*. 11. Ulusal Tesisat Mühendisliği Kongresi (pp. 17-20). http://www1.mmo.org.tr/etkinlikler/tesisat/etkinlik_bildirileri_detay.php?etkinlikkod=246&bilkod=1857
- Kehrer, M., Künz, H. M., & Sedlbauer, K. (2003). Ecological insulation materials-does sorption moisture affect their insulation performance? *Journal of Thermal Envelope and Building Science*, 26(3), 207-212. <https://doi.org/10.1177/109719603027869>
- Kennedy, C. E. (2002). *Review of mid-to high-temperature solar selective absorber materials*. <https://www.nrel.gov/docs/fy02osti/31267.pdf>
- Kim, Y., & Seo, T. (2007). Thermal performances comparisons of the glass evacuated tube solar collectors with shapes of absorber tube. *Renewable Energy*, 32(5), 772-795. <https://doi.org/10.1016/j.renene.2006.03.016>
- Koehn, R. K., Ondieki, H. O., Tonui, J. K., & Rotich, S. K. (2012). A steady state thermal model for photovoltaic/thermal (PV/T) system under various conditions. *International Journal of Scientific & Technology Research*, 1(11), 1-5. <http://www.ijstr.org/final-print/dec2012/A-Steady-State-Thermal-Model-For-Photovoltaicthermal-Pvt-System-Under-Variou-Conditions.pdf>

- Lu, S., Liang, R., Zhang, J., & Zhou, C. (2019). Performance improvement of solar photovoltaic/thermal heat pump system in winter by employing vapor injection cycle. *Applied Thermal Engineering*, 155, 135-146. <https://doi.org/10.1016/j.applthermaleng.2019.03.038>
- Malvi, C. S., Gupta, A., Gaur, M. K., Crook, R., & Dixon-Hardy, D. W. (2017). Experimental investigation of heat removal factor in solar flat plate collector for various flow configurations. *International Journal of Green Energy*, 14(4), 442-448. <https://doi.org/10.1080/15435075.2016.1268619>
- Masters, G. M. (2004). Photovoltaic materials and electrical characteristics. *Renewable and Efficient Electric Power Systems*. <https://doi.org/10.1002/0471668826.ch8>
- Moodley, P. (2021). *1 - Sustainable biofuels: opportunities and challenges*. In Sustainable Biofuels (pp. 1-20). Academic Press. <https://doi.org/10.1016/B978-0-12-820297-5.00003-7>
- Morice, C. P., Kennedy, J. J., Rayner, N. A., & Jones, P. D. (2012). Quantifying uncertainties in global and regional temperature change using an ensemble of observational estimates: The HadCRUT4 data set. *Journal of Geophysical Research: Atmospheres*, 117(D8). <https://doi.org/10.1029/2011JD017187>
- Nahar, A., Hasanuzzaman, M., & Rahim, N. A. (2017). Numerical and experimental investigation on the performance of a photovoltaic thermal collector with parallel plate flow channel under different operating conditions in Malaysia. *Solar Energy*, 144, 517-528. <https://doi.org/10.1016/j.solener.2017.01.041>
- Omeroğlu, G. (2018). Fotovoltaik-Termal (PV/T) sistemin sayısal (CFD) ve deneysel analizi. *Firat Üniversitesi Mühendislik Bilimleri Dergisi*, 30(1), 161-167. <https://dergi.firat.edu.tr/index.php/mbd/article/view/505>
- Ozakin, A. N., & Kaya, F. (2019). Effect on the exergy of the PVT system of fins added to an air-cooled channel: A study on temperature and air velocity with Ansys Fluent. *Solar Energy*, 184, 561-569. <https://doi.org/10.1016/j.solener.2019.03.100>
- Ozakin, A. N., Yakut, K., & Khalaji, M. N. (2020). Performance analysis of photovoltaic-heat pump (PV/T) combined systems: A comparative numerical study. *Journal of Solar Energy Engineering*, 142(2). <https://doi.org/10.1115/1.4045313>
- Pottler, K., Sippel, C. M., Beck, A., & Fricke, J. (1999). Optimized finned absorber geometries for solar air heating collectors. *Solar Energy*, 67(1-3), 35-52. [https://doi.org/10.1016/S0038-092X\(00\)00036-0](https://doi.org/10.1016/S0038-092X(00)00036-0)
- Rahman, S., Sarker, M. R. I., Mandal, S., & Beg, M. R. A. (2018). Experimental and numerical analysis of a stand-alone PV/T system to improve its efficiency. *Journal of Fundamentals of Renewable Energy and Applications*, 1, 28-33. <https://doi.org/10.4172/2090-4541.1000253>
- Richert, T., Riffelmann, K., & Nava, P. (2015). The influence of solar field inlet and outlet temperature on the cost of electricity in a molten salt parabolic trough power plant. *Energy Procedia*, 69, 1143-1151. <https://doi.org/10.1016/j.egypro.2015.03.184>
- Ritchie, H., & Roser, M. (2020). CO₂ and greenhouse gas emissions. *Our World In Data*. <https://ourworldindata.org/co2-and-other-greenhouse-gas-emissions>
- Rizk, J., & Chaiko, Y. (2008). Solar tracking system: More efficient use of solar panels. *World Academy of Science, Engineering and Technology*, 41(2008), 313-315. <https://www.semanticscholar.org/paper/Solar-Tracking-System%3A-More-Efficient-Use-of-Solar-Rizk-Chaiko/5594b5bbb72021eafd8a96452b6bb551d8208094>
- Sekhar, Y. R., Sharma, K. V., & Rao, M. B. (2009). Evaluation of heat loss coefficients in solar flat plate collectors. *ARPN Journal of Engineering and Applied Sciences*, 4(5), 15-19. <https://www.semanticscholar.org/paper/Evaluation-Of-Heat-Loss-Coefficients-In-Solar-Flat-Sekhar-Sharma/d2f0a067b0ade05d73ab14164400eb7fba3a9d5f>
- Song, Z., Ji, J., Zhang, Y., Cai, J., & Li, Z. (2021). Experimental and numerical investigation on a photovoltaic heat pump with two condensers: A micro-channel heat pipe/thermoelectric generator condenser and a submerged coil condenser. *Energy*, 122525. <https://doi.org/10.1016/j.energy.2021.122525>
- Tripanagnostopoulos, Y., Nousia, T. H., Souliotis, M., & Yianoulis, P. (2002). Hybrid photovoltaic/thermal solar systems. *Solar Energy*, 72(3), 217-234. [https://doi.org/10.1016/S0038-092X\(01\)00096-2](https://doi.org/10.1016/S0038-092X(01)00096-2)

- Yakut, R. (2021). A numerical study on determining the effect of original evaporator design on DX-SAHP system performance. *European Journal of Science and Technology*(28), 1052-1055. <https://doi.org/10.31590/ejosat.1012486>
- Yang, Y.-T., & Peng, H.-S. (2009). Numerical study of the heat sink with un-uniform fin width designs. *International Journal of Heat and Mass Transfer*, 52(15-16), 3473-3480. <https://doi.org/10.1016/j.ijheatmasstransfer.2009.02.042>
- Zadeh, P. M., Sokhansefat, T., Kasaeian, A. B., Kowsary, F., & Akbarzadeh, A. (2015). Hybrid optimization algorithm for thermal analysis in a solar parabolic trough collector based on nanofluid. *Energy*, 82, 857-864. <https://doi.org/10.1016/j.energy.2015.01.096>
- Zhang, X., Zhao, X., Shen, J., Xu, J., & Yu, X. (2014). Dynamic performance of a novel solar photovoltaic/loop-heat-pipe heat pump system. *Applied Energy*, 114, 335-352. <https://doi.org/10.1016/j.apenergy.2013.09.063>
- Zhou, J., Zhao, X., Ma, X., Qiu, Z., Ji, J., Du, Z., & Yu, M. (2016). Experimental investigation of a solar driven direct-expansion heat pump system employing the novel PV/micro-channels-evaporator modules. *Applied Energy*, 178, 484-495. <https://doi.org/10.1016/j.apenergy.2016.06.063>
- Zondag, H. A. (2008). Flat-plate PV-Thermal collectors and systems: A review. *Renewable and Sustainable Energy Reviews*, 12(4), 891-959. <https://doi.org/10.1016/j.rser.2005.12.012>
- Zwalnan, S. J., Caleb, N. N., Mangai, M. M., & Sanda, N. Y. (2021). Comparative analysis of thermal performance of a solar water heating system based on the serpentine and risers-head configurations. *Journal of Renewable Energy and Environment*, 8(2), 21-30. <https://doi.org/10.30501/jree.2020.251190.1150>